Biosensors and Bioelectronics 24 (2008) 558–565

Contents lists available at ScienceDirect

Biosensors and Bioelectronics

journal homepage: www.elsevier.com/locate/bios

Magnetic bead-based DNA detection with multi-layers quantum dots labeling for rapid detection of *Escherichia coli* O157:H7

Yi-Ju Liu [a], Da-Jeng Yao [a,*], Hwan-You Chang [b], Chien-Ming Liu [c], Chih Chen [c]

[a] *Institute of NanoEngineering and MicroSystems, National Tsing Hua University, Hsinchu 30013, Taiwan*
[b] *Institute of Molecular Medicine, National Tsing Hua University, Hsinchu 30013, Taiwan*
[c] *Department of Materials Science and Engineering, National Chiao Tung University, Hsinchu 30010, Taiwan*

ARTICLE INFO

Article history:
Received 16 March 2008
Received in revised form 5 May 2008
Accepted 4 June 2008
Available online 20 June 2008

Keywords:
DNA detection
Magnetic bead
Quantum dots
Biotin–streptavidin
Biotinlyted linker

ABSTRACT

This work demonstrated the feasibility of detecting 250 zM *Escherichia coli* O157:H7 *eae*A target DNA by using a magnetic bead-based DNA detection assay with designed labeling strategy within 40–60 min. The magnetic beads were used as the solid support for the binding probe and isolated the target DNA from the sample. The detection signals could be amplified from the multi-layers biotin–streptavidin conjugated quantum dots based on binding with specific designed biotinlyted linker. This assay method would provide a simple, rapid, and ultra-sensitive detection method for DNA or other biomolecular analysis.

1. Introduction

For detecting and quantitating biomolecules, the most common method still remains using fluorescence (Haugland et al., 2005; Lakowicz, 2006). The fluorescent probes have found extensive use in numerous biosensing applications including nucleic acid detection, immunoassays, cellular labeling, clinical or diagnostic assays, monitor of food or environment security and so on (Giepmans et al., 2006; Haugland et al., 2005; Lakowicz, 2006). However, many of the organic dye and protein-based fluorophores have serious chemical and photo-physical disadvantages, including pH dependence, high concentrations self-quenching, photo-bleaching susceptibility, short-term stability in liquid, narrow absorption windows coupled with broad emission spectra, and short fluorescent excitation lifetimes (Haugland et al., 2005; Lakowicz, 2006). Recently, quantum dots (QDs) are developed to be a novel nanomaterial which has special photo-physical properties for the assistance to develop a new production of powerful fluorescent biosensors. Since their first depiction in biological articles (Chan and Nie, 1998; Marcel et al., 1998), QDs have induced considerable of concern in the biosensing and bioanalysis community because of their particular fluorescent properties. Based on developed fundamental chemistry and materials science, the molecular biotechnology has allowed the engineering of advanced technical devices and the active substances for bioanalysis applications. Gradually, these fluorescent properties may avoid some of the disadvantages of conventional organic and protein-based fluorophores to help develop a new generation of biosensors. QDs properties used for biosensing include high quantum yields, broad absorption spectra coupled with narrow photo-luminescent emissions, resistance to both photobleaching and chemical degradation.

Because of the great photophysical properties, QDs (Chan and Nie, 1998; Marcel et al., 1998) has become a ideal nanomaterial especially for biosensing applications. Several properties of QDs, including narrow and size-tunable emission spectra, robust signal intensity, and resistance to photobleaching degradation, have made it become useful in fluorescent bioanalysis (Edgar et al., 2006; Ho et al., 2005). Lots of proteins, peptides, or other chemical molecules can be adhered to QDs surface, and these can impart some particular characteristic onto the QD-conjugate to generate functionality of formed multi-layers. On the other hand, the adhering multiple proteins through QDs can advance the aspiration to help for lowering the limitation of protein detection. Gradually, the size can permit the QDs to operate effectively both as a fluorophore and as a multifunctional nanomaterial for attachment of biomolecules or other materials.

Affinity biosensors are appeared by different types of transducing system, which applied to immunodetection and genodetection,

* Corresponding author. Tel.: +886 3 5715131 42850; fax: +886 3 5745454.
E-mail address: djyao@mx.nthu.edu.tw (D.-J. Yao).

0956-5663/$ – see front matter © 2008 Elsevier B.V. All rights reserved.
doi:10.1016/j.bios.2008.06.019

such as electrochemical, piezoelectric or magnetic ones. Based on a magnetic microbeads (MB) biofunctionalization transducer, enzymatic biosensors are usually amperometric, potentiometric or conductimetric. MB used in biomedical applications present generally a core–shell structure. Those microbeads have an inorganic core such as iron oxide, wrapped by an exterior layer of shell wall. The shell wall often consists of long chain organic ligands or inorganic/organic polymers. The adhesion of bioactive ligands to the surface of the exterior layer shell is the critical part of magnetic microbeads in bioapplication.

MB were also used in biomedical applications such as affinity biosensing (Gijs, 2004; Kerman et al., 2004; Sun et al., 2007), enzymatic biosensing (Shikida et al., 2006), and bio-bar codes detection system (Nam et al., 2004, 2003). Such microbeads used in biomedical applications present generally as a core–shell structure. Those microbeads have an inorganic core such as iron oxide, wrapped by an exterior layer of shell wall. The shell wall often consists of long chain organic ligands or inorganic/organic polymers. How to adhesive the bioactive ligands to the surface of the exterior layer shell would be the critical part of using magnetic microbeads in bioapplication?

Of all the recent technical advances in molecular biology, the PCR has been by far the most useful especially for nucleic acid amplification. The detection techniques have been employed for the detection of *Escherichia coli* O157:H7, including polymerase chain reaction (PCR) (Holland et al., 2000; Oberst et al., 1998; Witham et al., 1996), multiplex PCR (Fratamico et al., 1995; Wang et al., 2002), or real-time PCR assays (Bhagwat, 2003; Jothikumar and Griffiths, 2002; Sharma and Dean-Nystrom, 2003). However, there are several drawbacks, such as complexity, time consuming procedures, and narrow target. Recently, other detection methods were also developed, such as quartz crystal microbalance DNA sensor (Mao et al., 2006), piezoelectric immunosensor (Su and Li, 2004), surface plasmon resonance (SPR) (Fratamico et al., 1998; Kai et al., 2000), or electrochemical impedance (Ruan et al., 2002; Yang et al., 2004). The detection limit range was between 10^2 and 10^5 colony-forming units (CFU)/mL. Besides, for approaching PCR sensitivity, the Mirkin group has developed a unique signal amplification method based on the bio–bar code assay as a analytical tool for high sensitivity detection of DNA (Jaffrezic-Renault et al., 2007; Nam et al., 2004) and protein (Nam et al., 2003), and the sensitivity were 500 zM and 3 aM, respectively.

In this paper, we report a fluorescence signal amplification method for detecting target DNA in the very low concentration, which would rely on the novel signal labeling strategy through combination of MB and QDs. The target DNA was caught on the MB by probe hybridization and the signal were amplified by using multi-layers layers of QDs. We have showed the feasibility of offering 250 zM sensitivity by using this assay method, which will be shown.

2. Materials and methods

2.1. Chemicals and reagents

Magnetic beads (MBs, Dynabeads M-280, diameter 2.8 ± 0.2 μm, 12% iron oxide, Invitrogen) are commercial product which oligo $(dT)_{25}$ has already been modified on the surface of MBs for mRNA isolation originally. The 605 nm QDs streptavidin conjugate (Invitrogen), which is made from a nanometer-scale crystal of a semiconductor material (CdSe) and be coated with an additional semiconductor shell (ZnS) to improve the optical properties of the material, was used for fluorescence labeling. The target gene used in this study was associated with *E. coli* O157:H7 *eaeA* gene which encoded virulence factors so-called intimin. A 32 bp target DNA oligonucleotides (5′-GTC ACA GTT GCA GGC CTG GTT ACA ACA TTA TG-3′) was designed with reference to published sequence data for *eaeA* (Yu and Kaper, 1992). The capture probe DNA (5′-TGC AAC TGT GAC AAA AAA AAA A-3′) was designed to hybridize the target DNA near by the 5′ end of sequence. Forth more, the 3′ end of the capture probe DNA was designed to carry oligo $(dA)_{10}$ which were hybridized with oligo $(dT)_{25}$ in order to immobilize the target DNA on the surface of MBs. The signal probe DNA (biotin-5′-CAT AAT GTT GTA ACC AGG CC-3′) was designed to hybridize the target DNA near by the 3′ end of sequence, and the biotin would be used to bind with QDs through streptavidin on the surface. The target DNA must be detected under this labeling strategy if fluorescent intensity of QDs were detected. In order to improve the sensitivity, we tried to find more efficient ways to utilize the free streptavidin on the surface of QDs to generate more QDs binding on the surface of MB. Therefore, the biotinylated linker (BL, Biotin-5′-TGC GCC GTG GTA TAC CAC GGC GCA-3′) was designed as a bridge to link two QDs by biotin–streptavidin conjugation. Because the biotinylated linker was designed as hairpin sequence and to modify biotin molecular on its 5′ end, therefore, two such oligonucleotides were hybridized with each other as a double strand DNA which has both 5′ end biotin label. Thus, three-dimensional connections of BL and streptavidin on QDs would become a key issue to amplify the detection signal because there are more than 10 streptavidin–biotin binding sites for BL binding on each QDs (according to the product manual). Therefore, the designed probes were used to immobilize target DNA on the MB and to form multi-layers layers of QDs on the same beads by using BL for amplifying fluorescent signal. In addition, wash buffer (WB, 10 mM Tris–HCl, pH 7.5, 0.15 M LiCl, 1 mM EDTA) and binding buffer (BB, 20 mM Tris–HCl, pH 7.5, 1.0 M LiCl, 2 mM EDTA) were used in the whole following process.

2.2. DNA isolation and multi-layers QDs labeling

The schematic diagram of this detection method was shown in Fig. 1. The MBs was modified with oligo $(dT)_{25}$, and 605 nm QDs were modified with 10–15 streptavidin on the surface. For proving the feasibility of the multi-layers QDs labeling, in the first detection experiment, 10 μL MBs were washed with WB and resuspened in 100 μL BB, then mixed with adding 1 μL of 1 μM capture DNA, and placed at room temperature for 5 min. This step was used to make capture probe DNA locate on the MBs by oligo $(dA)_{10}$ hybridized with oligo $(dT)_{25}$. The next step was put them into the tube placed on the magnet for 2 min to carefully remove all the supernatant and wash several times by WB, then resuspended in 100 μL BB. One microliter of 300 nM target DNA was mixed the MBs, already hybridized with capture probe DNA, and kept at room temperature for 5 min. The controlled trial was only added MBs without any target DNA. After magnetically separate, wash and resuspend, the MBs were mixed with 1 μL of 300 nM signal probe DNA and also kept at room temperature for 5 min. With the same isolate and wash steps, the MBs were mixed with 1 μL 300 nM QDs and kept at room temperature for 5 min. After isolate and wash, the collected MBs were resuspended in 10 μL BB. Pick up 3 μL MB solution and took the optical and fluoresces image under fluorescence microscope, which would show the binding results of the first QDs layer. In order to form the multi-layers of QDs, 1 μL of 300 nM BL, which was treated with heating at 95 °C in 3 min and annealing at 50 °C in 3 min before use, was added into remained solutions. The total volume was controlled to be 100 μL by adding BB, and kept at room temperature for 5 min. Repeat the previous steps of BL and QDs binding, the multi-layers of QDs would be formed and the optical and fluoresces image was taken under fluorescence microscope.

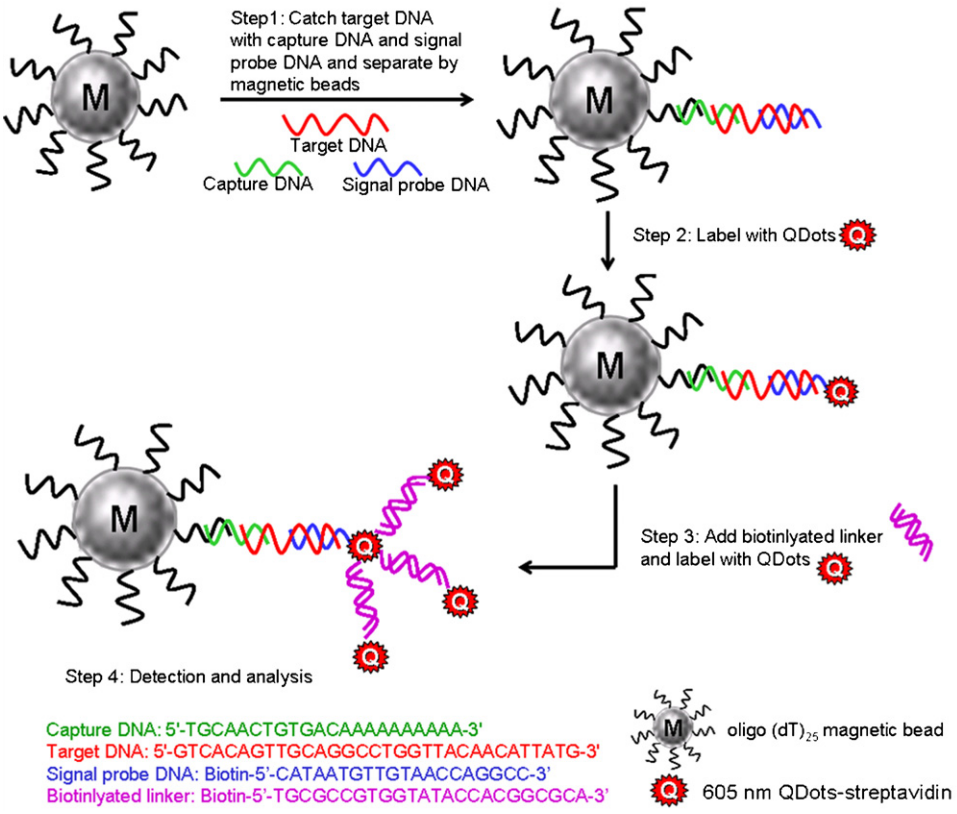

Fig. 1. The schematic diagram of this detection method: the magnetic bead-based assay with multi-layers quantum dots labeling.

2.3. Sensitivity and mismatch experiment

For the sensitivity measurement, three different concentration of the target DNA from 5 aM, 500 zM down to 250 zM were used, and their sample volume was 500 μL. The experiment steps were the same above description. Besides, for mismatch test, three oligonucleotides were used to make comparison with designed target DNA. There are two or ten mismatch bases, shown in Table 1. The concentrations of those analogic DNA are all 10 nM. After DNA isolation and labeling, each mismatch trial was treated with heating at different temperature including 35 °C, 40 °C, 45 °C, 50 °C and 51 °C for 3 min, respectively. And the optical and fluoresces images were also taken and analyzed.

2.4. Fluoresces image acquisition and data analysis

All images were taken using an Olympus BX51 microscope (40× objective) equipped with an RTKE digital camera. The fluorescence images were obtained by using blue excitation source ($\lambda_{ex} \sim 488$ nm) and exposure time is 0.2 s. The QDs fluorescent intensity evaluation was performed using ImageJ (the public software from National Institutes of Health). All taken fluorescence images were imported into ImageJ and normalized by using background signal. ImageJ can calculate the fluorescent intensity by using the same circle area on choosing every bead from the image. The top 50 strongest beads were chosen to obtain the average integrated density and standard deviation. The fluorescent intensity results subsequently were compiled for graphical analysis by SigmaPlot 2000 Demo (SPSS Inc.).

Table 1
DNA sequences used in this study

	Sequence (5′ → 3′)
Target DNA	GTCACAGTTGCAGGCCTGGTTACAACATTATG
Capture probe DNA	TGCAACTGTGAC$(A)_{10}$
Signal probe DNA	Biotin-CATAATGTTGTAACCAGGCC
Biotinylated linker	Biotin-TGCGCCGTGGTATACCACGGCGCA
Mismatch test	
2×	GTCACGGTTGCAGGCCTGGTTACGACATTATG
334×	GTCGTGGTTGCATATCTGGTTATGCTATTATG
10×	GTTACGGCTGTAGACTTGGCTACGACAGTACG

The underlined bases are mismatched nucleotide compared with designed target DNA.

3. Results and discussion

3.1. Multi-layers QDs labeling on the MB by DNA hybridize

In this experiment, we proved that the success of the target DNA isolated from the analyte solution by using the MB and the designed probes through the DNA hybridization. The signal probe and QDs associated through biotin–streptavidin conjugate and resulted in an optical signal. Furthermore, using the biotinylated linker as a bridge, the multi-layers QDs could be generated successfully and amplified the optical signals subsequently. For provide the practicable of multi-layers QDs labeling method, 300 nM target DNA were isolated successfully from the analyte solution by probe DNA hybridization and composed a MB-DNA-QDs sandwiched structure. In Fig. 2(a), the images showed that the fluorescent signals were amplified subsequently by three times QDs labeling. The "C" means that no target DNA was added in the whole analyte solution, which gave the fluorescent single from MB itself. The "Q1" means the target DNA labeled with the first layer QDs. Then BL and QDs reagent were added into the reaction mixture, which

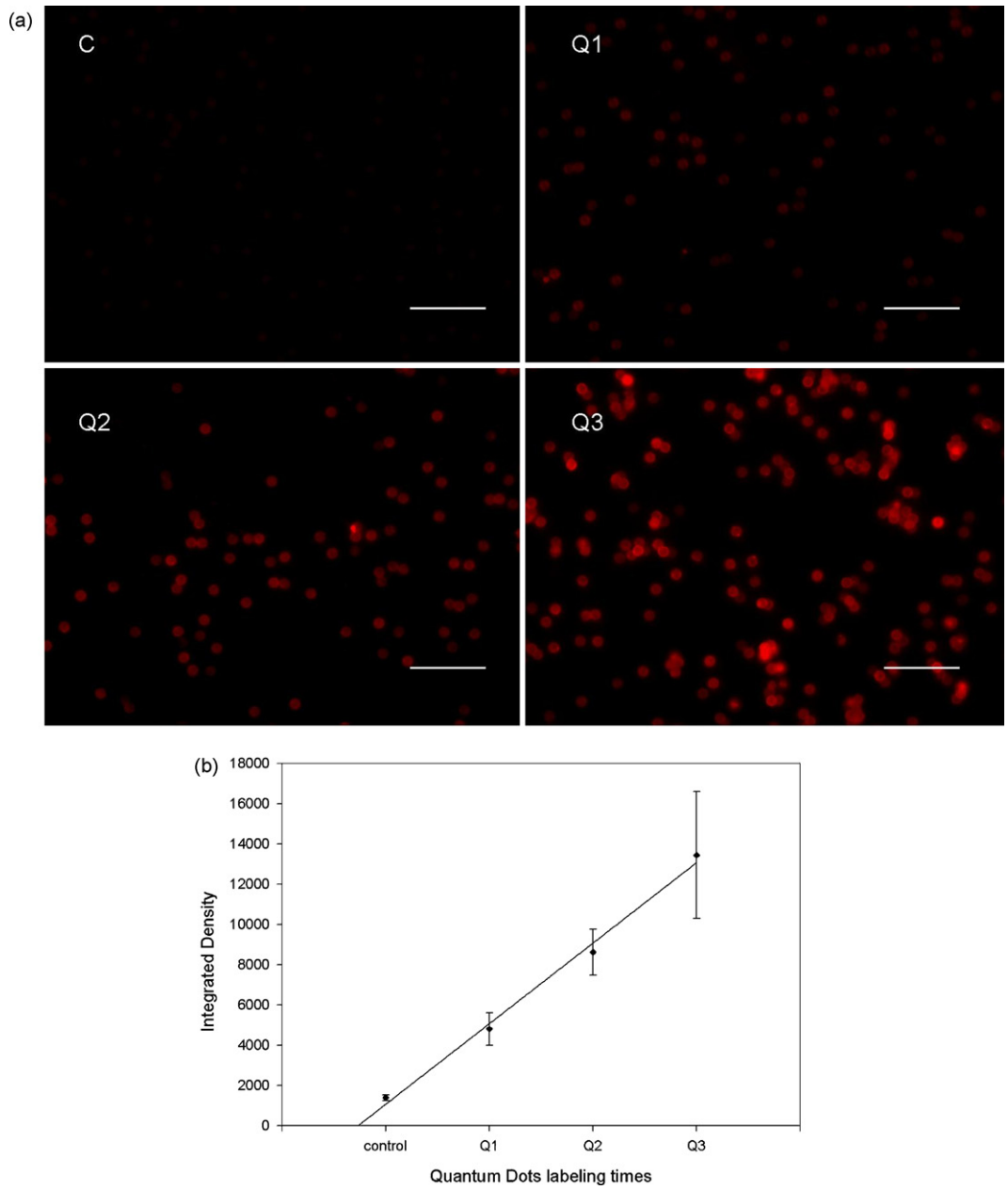

Fig. 2. The result of detect 300 nM target DNA using magnetic bead-based assay with multi-layers quantum dots labeling results. (a) The fluorescence images of target DNA detection with multi-layers QDs labeling. (b) Quantitative data of QDs intensities in different labeling times. (C: the controlled trial without target DNA; Q1: the first layer QDs labeling; Q2: the second layer QDs labeling; Q3: the third layer QDs labeling; scale bar: 20 μm).

was already labeled "Q1". The additional QDs would conjugate with the "free" streptavidin sites on the "Q1" by BL to form the second layer QDs. After second layer QDs was created, the fluorescent signal was amplified successfully, so call "Q2". As well as "Q2" labeling, "Q3" showed the third layer QDs on the MB, and the fluorescent signal of "Q3" became stronger than the one of "Q2". After analyzed the fluorescent intensity for each MB by ImageJ, the top 50th stronger intensity data were picked to calculate their average value and standard deviation. The results give good linearity ($R^2 = 0.9937$) from first layer QDs binding (Q1) up to third layer QDs binding (Q3), shown in Fig. 2(b). Because every layer of QDs and biotinlyted linkers were used based on the same concentration, we presume that all biomaterials could be consumed in the similar binding process. The average fluorescence intensity in the second layer was about one fold larger than first layer and so that the third's was larger than second's. Therefore, compared with the data shown in Fig. 2(b), the fluorescence intensity showed linear increasing dependence, and meanwhile, the QDs were binding orderly to form multi-layers on the MB. On the other hand, the larger deviation of the integrated density with the increase of labeling times, we presume that every magnetic bead captured the target DNA randomly from the beginning. With the increase of labeling times, those magnetic beads, which capture more target DNA from the beginning and shown lager fluorescence intensity, were binding more QDs and increase more fluorescence intensity. Although using a 488 nm excitation source would give conspicuous spectral overlap between the MB and 605 nm QDs (Agrawal et al., 2007), after three times QDs labeling, the fluores-

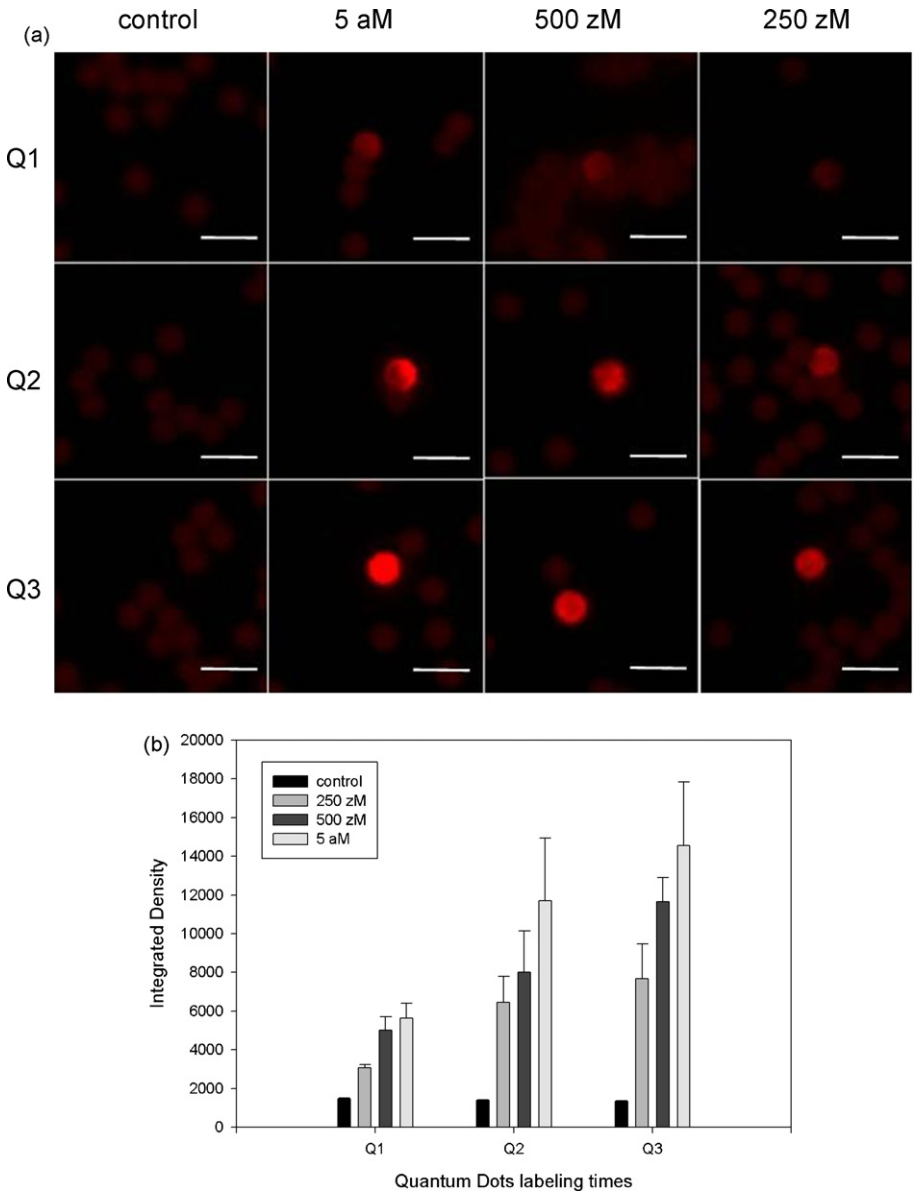

Fig. 3. The sensitivity results of 5 aM, 500 zM and 250 zM target DNA detection with multi-layers QDs labeling. (a) The fluorescence images of different concentration target DNA detection with multi-layers QDs labeling. (b) Quantitative data of QDs intensities in different labeling. Controlled trial was no target DNA in whole assay process (Scale bar: 5 μm).

cent signals could be obtained successfully because the fluorescent intensity of QDs is stronger than the background signal from the MB itself. Based on these results, the labeling strategy we reported was successful to amplify the fluorescence intensity. On the other hand, when designing the capture probe DNA with difference probe sequence and adding extra oligo (dA) tail, it would be flexible for detected difference organisms by using same oligo $(dT)_{25}$ MB.

3.2. Trial of sensitivity and mismatch discriminability

In the sensitivity measurement, three different concentrations of target DNA from 5 aM, 500 zM down to 250 zM have been detected and the fluorescence images shown in Fig. 3(a). After the first QDs labeling, both of 5 aM and the 500 zM trials showed a slightly fluorescence signal on the MB. Following the second and third QDs labeling, the fluorescence signals were amplified successfully. On the other hand, the 250 zM target DNA showed only little fluorescence signal after first labeling due to its low concentration, however, the fluorescence signals became clear by using second and third QDs labeling. The controlled trial was also showed no fluorescent as forward description. The integrated density results, shown in the Fig. 3(b), were also showed that the increased progressively with multi-layers QDs labeling. Therefore, after three times labeling, the fluorescence intensity were shown that a 250 zM concentration of the target DNA could become detectable through the multi-layers QDs labeling method.

In the mismatch trial, the MB–DNA–QDs complex was heated at different temperatures for 3 min, the results showed that the optical signal of 2× (two base mismatch) disappeared at 51 °C, and the optical signal of 334× (ten bases mismatch, partially bases separated)

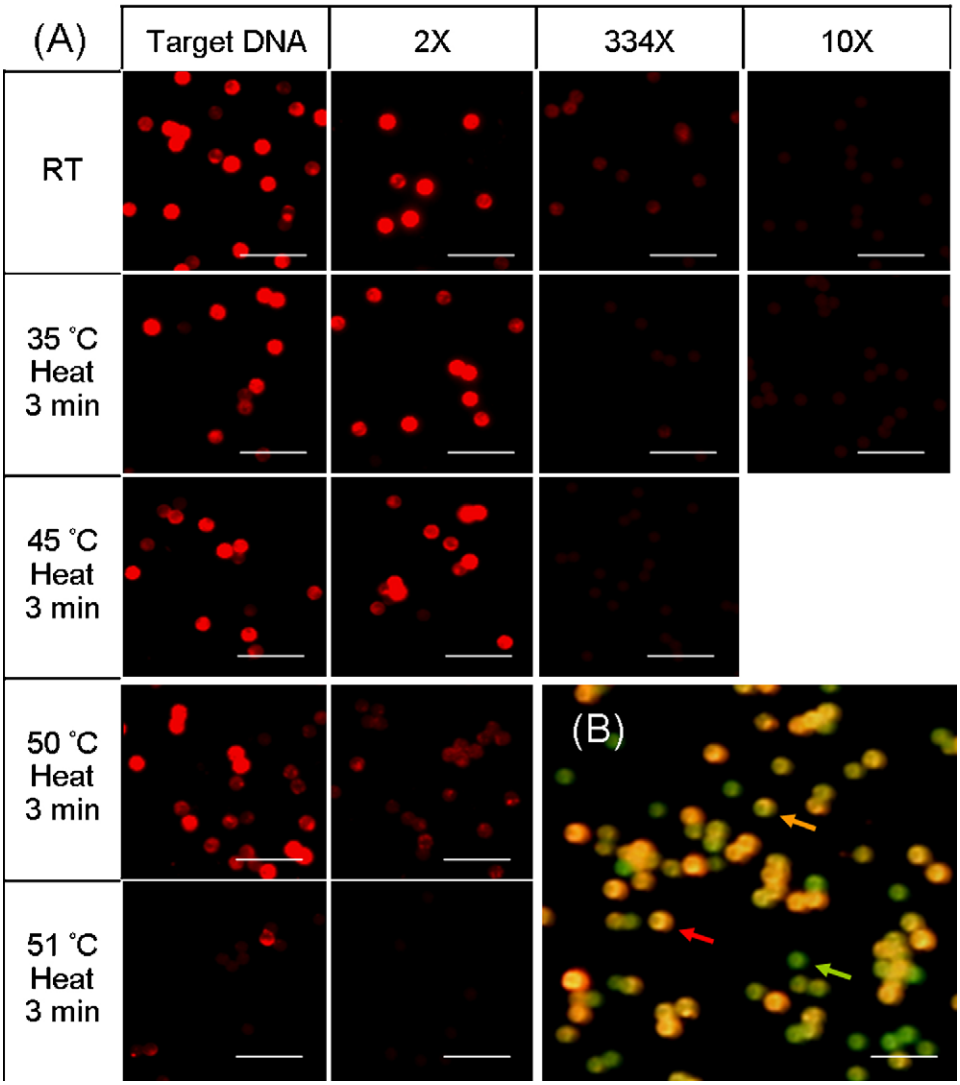

Fig. 4. The fluorescence images of different mismatch results. (A) The optical signal of 2× (two base mismatch) disappeared at 51 °C, and the optical signal of 334× (ten bases mismatch, partially bases separated) and 10× (ten bases mismatch, all bases separated) disappeared at 45 °C and 35 °C, respectively. The perfect match target DNA still kept obvious fluorescence signals. (B) The digital image was taken directly under fluorescence microscope. Based on the binding probability, MBs would catch different number of target DNA. The green arrow showed the original fluorescence signal of MB only. The orange arrow showed the fluorescence signal of MB with binding few of target DNA that showed the middle fluorescence signal. The red arrow the fluorescence signal of MB with binding lots of target DNA that showed the stronger fluorescence signal (Scale bar: 15 μm) (For interpretation of the references to color in this figure legend, the reader is referred to the web version of the article).

and 10× (ten bases mismatch, all bases separated) disappeared at 45 °C and 35 °C, respectively. Although the fluorescent signal of target DNA (preface match) became weak at 51 °C, however, it still has the discriminability with mismatch elements, shown in Fig. 4(A). Besides, because of the binding probability between MBs and QDs, each MB would bind different number of target DNA to generate different intensity of QDs fluorescent signals, digital image shown in Fig. 4(B). For confirming the binding phenomenon, the TEM image showed the interaction of QDs bound on the surface of MB, shown on Fig. 5. The MBs has good suspension and without the aggregation in the reaction solution whether in high or low DNA concentration experiment which executed in this study. The MBs shown clustery in the TEM image should because of the solution evaporated to aggregate the MBs. In the TEM image, the Fig. 5(D) showed the second QDs binding on the first QDs. It is necessary to explore the more appropriate detection method to confer the forming of the multi-layers structure and to compare the relationship between the fluorescence intensity and QDs numbers.

The immuno-compromised patients, mostly children or very old people, were mostly the infected sensitive members. The infective dose of *E. coli* O157:H7 is 50–100 organisms (Singleton, 2004) and the satisfactory microbiological quality with the acceptable range being 20–<100 CFU/g (Gilbert et al., 2000). Ready-to-eat food should be free from *E. coli* O157 and other verocytotoxigenic *E. coli* (VTEC) organisms in the UK (Gilbert et al., 2000). The sensitivity of traditional detection method in the *E. coli* O157:H7 is between 10^2 and 10^5 CFU/mL, and it spends tens of minutes up to several hours. In our study, the limitation of multi-layers QDs labeling is 250 zM, about 150 molecules target DNA per milliliter. Although the sensitivity was not good enough for the infective dose, however, by concentrated target DNA binding range, such as using single bead or narrow down the detection area, lower DNA concentration molecular detection could be achieved by using our labeling strategy.

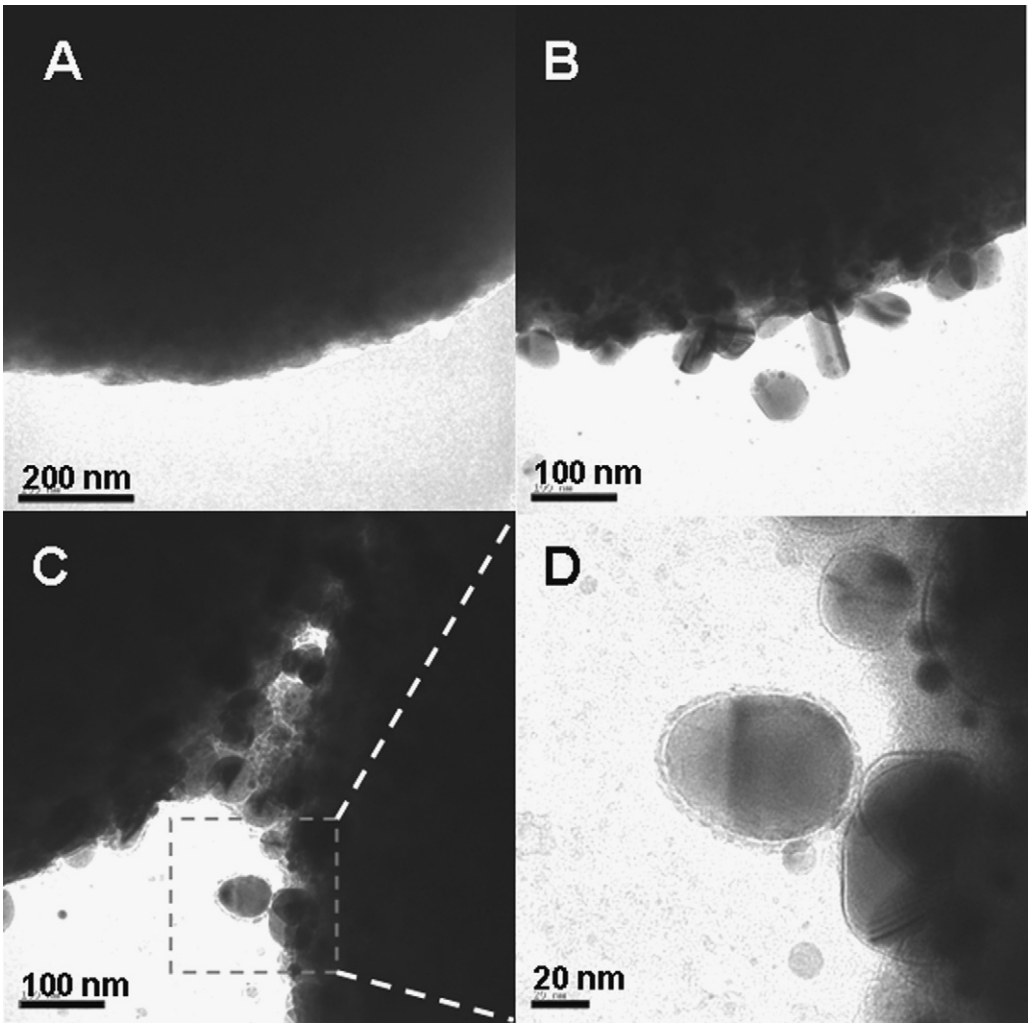

Fig. 5. TEM images of QDs binding on the surface of magnetic bead. (a) The magnetic bead without QDs binding, (b and c) are QDs binding on the magnetic bead after labeling assay, and (d) the zoom-in image for QDs binding on the surface of magnetic bead.

4. Conclusions

In this study, we reported a labeling strategy to amplify the fluorescence intensity and successfully demonstrate the feasibility of detecting 250 zM target DNA with magnetic beads and multi-layers quantum dots. This labeling method could be combined with bioanalysis sensor such as microfluidic devices for speedy detection of the disease or to be applied as a facile tool for observation of single biomolecular behavior under fluorescence microscope. On the other hand, using multi-layers QDs labeling, low concentration biomolecular such as RNA, protein, or virus could be observed. Furthermore, by using multicolor functionalized quantum dots as probes, this labeling method could be considered to expand the penitential to be improved, not only for oligonucleitide and DNA but also for protein or other biomolecular biosenescing method on bead-based or chip-based assay.

Acknowledgment

The authors would like to thank the National Science Council of ROC for financial support through grant NSC96-2221-E007-128-MY3.

References

Agrawal, A., Sathe, T., Nie, S., 2007. Journal of Agricultural and Food Chemistry 55 (10), 3778–3782.
Bhagwat, A.A., 2003. International Journal of Food Microbiology 84 (2), 217–224.
Chan, W.C.W., Nie, S., 1998. Science 281 (5385), 2016.
Edgar, R., McKinstry, M., Hwang, J., Oppenheim, A.B., Fekete, R.A., Giulian, G., Merril, C., Nagashima, K., Adhya, S., 2006. Proceedings of the National Academy of Sciences 103 (13), 4841–4845.
Fratamico, P.M., Sackitey, S.K., Wiedmann, M., Deng, M.Y., 1995. Journal of Clinical Microbiology 33 (8), 2188–2191.
Fratamico, P.M., Strobaugh, T.P., Medina, M.B., Gehring, A.G., 1998. Biotechnology Techniques 12 (7), 571–576.
Giepmans, B.N.G., Adams, S.R., Ellisman, M.H., Tsien, R.Y., 2006. The Fluorescent Toolbox for Assessing Protein Location and Function. American Association for the Advancement of Science, pp. 217–224.
Gijs, M.A.M., 2004. Microfluidics and Nanofluidics 1 (1), 22–40.
Gilbert, R.J., de Louvois, J., Donovan, T., Little, C., Nye, K., Ribeiro, C.D., Richards, J., Roberts, D., Bolton, F.J., 2000. Communicable Diseases Public Health 3 (3), 163–167.
Haugland, R.P., Spence, M.T.Z., Johnson, I.D., Basey, A., 2005. Molecular Probes.
Ho, Y.P., Kung, M.C., Yang, S., Wang, T.H., 2005. Nano Letters 5 (9), 1693–1697.
Holland, J.L., Louie, L., Simor, A.E., Louie, M., 2000. Journal of Clinical Microbiology 38 (11), 4108.
Jaffrezic-Renault, N., Martelet, C., Chevolot, Y., Cloarec, J.P., 2007. Sensors 7, 589–614.
Jothikumar, N., Griffiths, M.W., 2002. Applied and Environmental Microbiology 68 (6), 3169–3171.
Kai, E., Ikebukuro, K., Hoshina, S., Watanabe, H., Karube, I., 2000. FEMS Immunology and Medical Microbiology 29 (4), 283–288.
Kerman, K., Matsubara, Y., Morita, Y., Takamura, Y., Tamiya, E., 2004. Science and Technology of Advanced Materials 5 (3), 351–357.

Lakowicz, J.R., 2006. In: Lakowicz, J.R. (Ed.), Principles of Fluorescence Spectroscopy. Springer, Berlin, ISBN 0-387-31278-1.
Mao, X., Yang, L., Su, X.L., Li, Y., 2006. Biosensors and Bioelectronics 21 (7), 1178–1185.
Marcel, B.J., Moronne, M., Gin, P., Weiss, S., Alivisatos, A.P., 1998. Science 281, 2013–2016.
Nam, J.M., Thaxton, C.S., Mirkin, C.A., 2003. Science 301 (5641), 1884–1886.
Nam, J.M., Stoeva, S.I., Mirkin, C.A., 2004. Journal of the American Chemical Society 126 (19), 5932–5933.
Oberst, R.D., Hays, M.P., Bohra, L.K., Phebus, R.K., Yamashiro, C.T., Paszko-Kolva, C., Flood, S.J., Sargeant, J.M., Gillespie, J.R., 1998. Applied and Environmental Microbiology 64 (9), 3389.
Ruan, C., Yang, L., Li, Y., 2002. Analytical Chemistry (Washington) 74 (18), 4814–4820.
Sharma, V.K., Dean-Nystrom, E.A., 2003. Veterinary Microbiology 93 (3), 247–260.
Shikida, M., Takayanagi, K., Honda, H., Ito, H., Sato, K., 2006. Journal of Micromechanics and Microengineering 16 (9), 1875–1883.
Singleton, P., 2004. Bacteria in Biology, Biotechnology and Medicine, 6th ed. Wiley.
Su, X.L., Li, Y., 2004. Biosensors and Bioelectronics 19 (6), 563–574.
Sun, Y., Bai, Y., Song, D., Li, X., Wang, L., Zhang, H., 2007. Biosensors and Bioelectronics 23 (4), 473–478.
Wang, G., Clark, C.G., Rodgers, F.G., 2002. Journal of Clinical Microbiology 40 (10), 3613.
Witham, P.K., Yamashiro, C.T., Livak, K.J., Batt, C.A., 1996. Applied and Environmental Microbiology 62 (4), 1347–1353.
Yang, L., Li, Y.B., Erf, G.F., 2004. Analytical Chemistry (Washington) 76 (4), 1107–1113.
Yu, J., Kaper, J.B., 1992. Molecular Microbiology 6 (3), 411–417.